Electrochemical Impedance Spectroscopy (EIS) Analysis of Film Formation in CO_2 Corrosion

by

Abid Haq bin Abdul Aziz

Dissertation submitted in partial fulfillment of
the requirements for the
Bachelor of Engineering (Hons)
(Mechanical Engineering)

JUNE 2010

Universiti Teknologi PETRONAS
Bandar Seri Iskandar
31750 Tronoh
Perak Darul Ridzu

CERTIFICATION OF APPROVAL

Electrochemical Impedance Spectroscopy (EIS) Analysis of Film Formation in CO_2 Corrosion

by

Abid Haq bin Abdul Aziz

A project dissertation submitted to the
Mechanical Engineering Programme
Universiti Teknologi PETRONAS
in partial fulfillment of the requirement for the
BACHELOR OF ENGINEERING (Hons)
(MECHANICAL ENGINEERING)

Approved by,

_____

Assoc. Prof. Ir. Dr. Mokhtar Che Ismail

UNIVERSITI TEKNOLOGI PETRONAS

TRONOH, PERAK

JUNE 2010

CERTIFICATION OF ORIGINALITY

This is to certify that I am responsible for the work submitted in this project, that the original work is my own except as specified in the references and acknowledgements, and that the original work contained herein have not been undertaken or done by unspecified sources or persons.

_____

ABID HAQ BIN ABDUL AZIZ

ABSTRACT

Corrosion is defined as the deterioration of material, usually metal, by a chemical or electro-chemical reaction with its environment. In oil and gas industry, CO_2 corrosion is one of the recognized problems particularly in production, transportation facilities and the material selection process. In the application of carbon steel, it has become a main concern because of its high corrosion rate and the formation of protective iron carbonate (FeCO3) film layers. Current models often over-predict CO_2 corrosion rates for wet gas and oil transport systems. One of the main reasons for this is the fact that the formation of corrosion product scales is not properly taken into account. The objective of this project is to study and analyze on CO_2 corrosion rate together with the formation of protective iron carbonate (FeCO3) film layers. Laboratory experiments of CO_2 corrosion on carbon steel in natural and induced film forming environment with Fe^{2+}concentration (c_{Fe}^{2+}) of 0 and 50 ppm respectively, are conducted, in order to understand the $FeCO_3$ film formation. The study is conducted at temperatures of 25°C and 80°C at pH 5.5, partial pressure of CO_2 at 1 bar and stagnant conditions to observe how these parameters affect the CO_2 corrosion rate and formation of $FeCO_3$ film layers. Two electrochemical test techniques namely Electrochemical Impedance Spectroscopy (EIS) and Linear Polarization Resistance (LPR) are used. From the EIS technique, in the natural film forming environment, as the temperature increases from 25°C to 80°C, the corrosion rate decreases from 1.18 mm/year to 0.32 mm/year. In contrast, for the induced film forming environment, the corrosion rate decreases from 1.38 mm/year at temperature of 25°C to 0.99 mm/year at temperature of 80°C. Meanwhile, for LPR technique, in the natural film forming environment, as the temperature increases from 25°C to 80°C, the corrosion rate decreases from 1.54 mm/year to 0.31 mm/year. In contrast, for the induced film forming environment, the corrosion rate decreases from 0.25 mm/year at temperature of 25°C to 0.18 mm/year at temperature of 80°C. It has been observed that the corrosion rate is relatively lower in induced film forming environment since the increase of Fe^{2+}concentration results in higher supersaturation.

ACKNOWLEDGEMENTS

Firstly, thank you Allah S.W.T, the Most Gracious and the Most Merciful for His blessings throughout the process of completing this project. The author would also like to thank his FYP supervisor, Assoc. Prof. Ir. Dr. Mokhtar Che Ismail, for his able guidance, advice and encouragement. The author wishes to convey his earnest thanks to the following postgraduate students; Ms. Sarini bt. Mat Yaakob, Ms. Anis Amilah bt. Abdul Rahman, Mr. Martin Choirul Fatah and Mr. Yuli Panca Asmara where they have shared their valuable thoughts and knowledge in the process of completing this project. Besides that, the author wishes special thanks to the Mechanical Laboratory Technicians particularly Mr. M Faisal Ismail for his help and assistance during sample preparation and Mr. Irwan Othman in using the SEM facilities. The author is also very grateful to his fellow colleague Mr. Zafrin bin Zainal Azmi, whom had given much cooperation during the earlier stages of the project. Not forgetting, a word of thanks also goes to the author's beloved family, Mr. Abdul Aziz bin Abdul Kadir, Madam Zawiyah Hassan, Dalilah bt. Abdul Aziz and Irman Hafiz bin Zulkifli for their support which has definitely motivated the author to complete this project. Lastly, the author would like to thank all those people who have contributed in one way or another, directly or indirectly in the process of carrying out this project.

TABLE OF CONTENTS

LIST OF FIGURES

LIST OF TABLES

CHAPTER 1
INTRODUCTION

1.1 Background of Study

Corrosion is defined as the deterioration of material, usually metal, by a chemical or electro-chemical reaction with its environment. It is a natural act of metals trying to return to their lowest level of energy.

According to Van Hunnik [1], Reliable prediction and control of corrosion is the key to cost-effective and safe design of facilities for the gas and oil industry. For example, current tools for the prediction of CO corrosion in pipelines are still based on "worst case" assumptions, which may lead to unnecessary operational expenditures to combat potential corrosion. These extra costs can stem from the use of expensive corrosion resistant steels, too much corrosion allowance (extra steel wall thickness), or application of a corrosion inhibitor. One area where there might be scope for design improvements concerns the description of the formation of corrosion product layers (scaling), which may limit the progress of internal pipeline corrosion. Currently the potential protective properties of scales cannot be taken into account in predictive models as adequate understanding of their stability and reliability, e.g. under fluid flow conditions, is lacking.

In facilities for oil and gas production, handling and transport, iron carbonate is often the main corrosion product. It forms at the wall of a pipeline if the product of ferrous ion concentration and carbonate ion concentration, exceeds the solubility product. The precipitation kinetics is known to be relatively slow and allows much higher ferrous ion concentrations than would be dictated by thermodynamic equilibrium. This condition is

known as supersaturation. Literature on the precipitation kinetics of is rather limited and additional corrosion experiments would have to be carried out. This information enabled the development of an improved description of the kinetics. A number of potential application examples, for which knowledge of the iron carbonate precipitation process is relevant, will be dealt with [1].

Linear Sweep Voltammetry (LSV), Electrochemical Impedance Spectroscopy (EIS) and Electrochemical Noise (ECN) are among the electrical characterization methods available. However, Electrochemical Impedance Spectroscopy (EIS) that has been proven to be an effective technique for measuring corrosion rate will be used in this project and further analysis will be carried out on the formation of $FeCO_3$ film layers.

1.2 Problem Statement

Current models often over-predict CO_2 corrosion rates for wet gas and oil transport systems. One of the main reasons for this is the fact that the formation of corrosion product scales is not properly taken into account. However, for this project, study and analysis on CO_2 corrosion would be conducted to obtain a deeper understanding on the formation of corrosion product scales in which under certain condition, stable and protective corrosion product will be formed.

1.2.1 Problem Identification

The precipitation kinetics of $FeCO_3$ is known to be relatively slow. Therefore, many experiments will need to be conducted throughout the time frame given to further understand the $FeCO_3$ precipitation process.

1.2.2 Significance of the Project

The ultimate aim of this study on precipitation kinetics is to enable the prediction of the formation of protective corrosion product layers and the resulting reduction of the corrosion rate. By combining models for corrosion rate and precipitation kinetics the appearance of $FeCO_3$ layers can be predicted. This is essential to determine whether $FeCO_3$ film formation is protective, semi-protective or not protective. Simultaneously, the output of this project is intended to help the material selection process in the oil and gas industry. By all means, it is already known that a bad material selection process may lead to unnecessary extra capital or operational expenditures to combat potential corrosion. These extra costs can stem from the use of expensive corrosion resistant steels, too much corrosion allowance (extra steel wall thickness), or application of a corrosion inhibitor.

1.3 Objectives and Scope of Study

The main objectives for this project are:

- To study and analyze the CO_2 corrosion rate and formation of $FeCO_3$ film layers. To conduct laboratory experiment in CO_2 environment and measure the CO_2 corrosion rate on the carbon steel, using Electrochemical Impedance Spectroscopy (EIS) technique.

- To compare the effect of temperature on the corrosion rate of carbon steel in natural and induced film forming environment.

1.4 Scope of the Project

The objective of this project is support by the following scope of study:

- To study and analyze the formation $FeCO_3$ film layers and CO_2 corrosion rate using the EIS technique in CO_2 environment.
- The parameters that will be varied throughout this project are temperature and the concentration of $Fe2^+$ only. The other affecting parameters will be set as constant.

1.5 Relevancy of the Project

A thorough understanding on the effect of $FeCO_3$ film formation on CO_2 corrosion will provide useful information thus help in having reliable prediction in the formation of protective corrosion product layers, which is able to lead us in a cost-effective and safe design of production and transportation facilities used in the oil and gas industry.

1.6 Feasibility of the Project

The project is initiated by collecting materials such as books, journals and technical papers specifically on CO_2 corrosion of carbon steel and $FeCO_3$ film formation. Research will be conducted by stages to ensure better understanding is captured. This project will then focus on conducting laboratory experiments on carbon steel in CO_2 environment. Study and analysis will be emphasized more on the behavior of $FeCO_3$ film formation and the effect of CO_2 corrosion rate on carbon steel.

CHAPTER 2
LITERATURE REVIEW

2.1 Overview of CO_2 Corrosion

Carbon dioxide (CO_2) corrosion is one of the most important concerns in the oil and gas industry [2]. The capital and operational expenditures and health, safety and environment of the oil and gas industry are enormously affected by corrosion [3]. The study of CO_2 corrosion rate and iron carbonate ($FeCO_3$) film formation as one of the corrosion products has been carried out rapidly in the last 30 years to develop the understanding and modeling the kinetics of $FeCO_3$ precipitation process.

The presence of CO_2 in solution leads to the formation of a weak carbonic acid (H_2CO_3) which drives CO_2 corrosion reactions [4]. The initiating process is presented by the reaction shown in equation (2.1).

$$CO_2 + H_2O \leftrightarrow H_2CO_3 \quad (2.1)$$

The following corrosion process is controlled by three cathodic reactions and one anodic reaction. The cathodic reactions, include (2.1a) the reduction of carbonic acid into bicarbonate ions, (2.1b) the reduction of bicarbonate ions, and (2.1c) the reduction of hydrogen ions.

$$2H_2CO_3 + 2e^- \rightarrow H_2 + 2HCO_3^- \quad (2.1a)$$

$$2HCO_3^- + 2e^- \rightarrow H_2 + 2CO_3^{2-} \quad (2.1b)$$

$$2H^+ + 2e^- \rightarrow H_2 \quad (2.1c)$$

The anodic reaction significant in CO_2 corrosion is the oxidation of iron to ferrous (Fe^{2+}) ion given in equation (3).

$$Fe \rightarrow Fe^{2+} + 2e^- \quad (2.2)$$

This corrosion reaction promotes the formation of $FeCO_3$ which can form along a couple of reaction paths. First, it may form when ferrous ions react directly with carbonate ions as shown in equation (2.3). However, it can also form by the two processes shown in equations (2.4a, 2.4b). When ferrous ions react with bicarbonate ions, ferrous iron bicarbonate forms which subsequently dissociates into iron carbonate along with carbon dioxide and water.

$$Fe^{2+} + CO_3^{2-} \rightarrow FeCO_3 \quad (2.3)$$

$$Fe^{2+} + 2HCO_3^{-} \rightarrow Fe(HCO_3)_2 \quad (2.4a)$$

$$Fe(HCO_3)_2 \rightarrow FeCO_3 + CO_2 + H_2O \quad (2.4b)$$

Precipitation of iron carbonate on the surface of the metal decreases the corrosion rate by acting as a diffusion barrier for the corrosive species to travel to the metal surface by blocking few areas on the steel surface and preventing electrochemical reactions from happening on the surface [1]

Whilst there is some debate about the mechanism of CO_2 corrosion in terms of which dissolved species are involved in the corrosion reaction, it is evident that the resulting corrosion rate is dependent on the partial pressure of CO_2 gas which will determine the solution pH and the concentration of dissolved species [2]. Next, the parameters affecting CO2 corrosion environment will be discussed briefly.

2.1.3 Parameters Affecting CO_2 Corrosion

There are several parameters that affect corrosion rate in CO_2 environment. The chemistry of both formation and dissolution of corrosion products, rates of chemical reactions and transportation rates of species involved in CO_2 corrosion can be affected by the following parameters:

1) Temperature

Prior to any $FeCO_3$ film layers formation the corrosion rate increases with temperature. However, at temperature of 60°C and higher, corrosion rate will start decreases as very protective $FeCO_3$ film layers already start to form.

2) CO_2 partial pressure

In the conditions where the formation of protective $FeCO_3$ film layers is favorable, increased CO_2 partial pressure will decrease corrosion rate. Given that the pH is high enough, higher CO_2 partial pressure leads to an increase in CO_3^{2-} concentration and a higher supersaturation which accelerates precipitation and $FeCO_3$ film layers formation.

3) pH

The pH has a strong influence on the conditions leading to the formation of protective $FeCO_3$ film layers. High pH results in a decreased solubility of $FeCO_3$, increased supersaturation and consequently higher precipitation rate which leads to the decrease in corrosion rate.

4) Fe^{2+}concentration

The increase of Fe^{2+}concentration results in higher supersaturation, which consequently accelerates the precipitation rate and reduces the corrosion rate.

5) Flow velocity

High flow velocity leads to increase in corrosion rate as it transports Fe^{2+} ions away from carbon steel surface, leads to a lower concentration of Fe^{2+} ions at carbon steel surface and prevents the formation of protective $FeCO_3$ film layers.

2.2 $FeCO_3$ Film Formation

Table 2.1: Characteristics of Corrosion Films

Characteristics of Corrosion Films			
Corrosion Film Class	Temperature Range of Formation (°C)	Characteristics Nature	Growth Habit and Composition
Transparent	Forms at room temperature and below	<1μm, transparent. Once formed, it is very protective	Forming fast as room temperature reduces to < room temperature mainly consisting Fe and Oxygen
Iron Carbide, (Fe_3C)	No range	< 100 μm thick, metallic conductive and non-adherent	Spongy and brittle, Consisting Fe n C
Iron Carbonate ($FeCO_3$)	Min. requirement in laboratory conditions (50°C to 70°C)	Adherent, productive and non conductive	Cubic Morphology consisting Fe, C and O
Iron Carbonate ($FeCO_3$) + Iron Carbide (Fe_3C)	Maximum temperature is 150°C. Higher temperatures have not been studied	All depends on how the two film blend together	Consisting of ferrous carbide and ferrous carbonate

Hence, based on extensive observations made by any workers, corrosion films in the 5°C to 150°C temperature range in water containing CO_2 can generally be divided into four classes which are:

- Transparent films.
- Iron carbide films.
- Iron carbonate films and
- Iron carbonate + Iron carbide films.

Their overall characteristics are summarized in Table 1. [2]

The formation of $FeCO_3$ film layers will eventually lead to the reduction of the corrosion rate. However, the exact corrosion reduction is difficult to predict in view of many factors involved such as type of steel, the fluid flow velocity, temperature, CO_2 partial pressure, pH and Fe^{2+}concentration. It is clear that a full description of the influence of precipitation on corrosion rate is far too complicated. However, prediction of the corrosion rate reduction may be possible under specific conditions. A further study shows that corrosion can only be reduced if the precipitation rate is of the order of the corrosion rate [1].

In order to predict the CO_2 corrosion rate successfully, the following aspects should be clarified such as:

- Protective $FeCO_3$ film formation.
- The stability of these layers.
- Adherence to the steel surface of these layers and
- Repair of damaged scales.

The ability of damaged scales to self-repair has greatly influenced the reliability of protective $FeCO_3$ film formation [5].

2.2.1 Effect of Surface Films in CO2 Corrosion

In CO2 Corrosion when the concentration of FeCO3, exceeds the solubility limit, they combine to form iron carbonate films on the steel surfaces as mentioned above .Therefore, high saturation near surface is needed for the formation of protective films. Once the film is formed, it will remain protective at a much lower supersaturation [6]. In obtaining a successful protection, the film must be adherent and cover the whole surface. Temperature strongly influences the conditions needed to form protective iron carbonate layers. At lower temperatures (<60°C) the solubility of $FeCO_{3\ is}$ high and the precipitation rate is slow and protective films will not form unless the pH is increased.

The precipitation rate of $FeCO_3$ has been described as slow and temperature dependent process and even under supersaturated conditions, high corrosion rates can maintain for weeks until protective iron carbonate layers are formed, specifically at low temperatures. Furthermore, in flow systems corrosion films obviously can grow for months without giving protection unless the steel is exposed to stagnant or "wet" conditions [7]. During a few days stagnation, corrosion products can accumulate on the steel surface and form protective films. Thus, kinetics of $FeCO_3$ precipitation seems to be a controlling factor for the protectiveness of the corrosion product layer. At higher temperature, the $FeCO_3$ solubility is reduced and the precipitation rate is much faster thus allowing the formation of iron carbonate films.

However, the morphology of iron carbonate scales depends not only on the temperature, but also on the pH and and the CO2 partial pressure as well. At higher pH values (>6.5), protective iron carbonate films can also form at room temperature [8, 9]. It has also been found that supersaturation is an important factor for film growth and the protectiveness of the film [10].

2.3 Electrochemical Measurement Techniques

In this project, the effect of $FeCO_3$ film formation on CO_2 corrosion rate will be analyzed using EIS and LPR and all the data obtained from the experiments would assist in providing a reliable prediction on the behavior of CO_2 corrosion that will leads to cost-effective and safe design of production and transportation facilities used in the oil and gas industry.

2.3.1 Electrochemical Impedance Spectroscopy (EIS)

An important advantage of EIS technique over other laboratory techniques is the possibility of using very small amplitude signals without significantly disturbing the properties being measured. In recent years, EIS technique has found widespread applications in the field of characterization of materials. It is routinely used in the characterization of coatings, batteries, fuel cells and corrosion phenomena. It has also been used extensively as a tool for investigating mechanisms in electrodeposition, electrodissolution, passivity and corrosion studies.

An electrochemical process may often be modeled by linear circuit elements such as resistors, capacitors, and inductors. For example, the corrosion reaction itself can often be modeled by one or more resistors. The ability to model a corrosion process in this manner gives rise to one practical attribute of the electrochemical impedance technique. Simple AC circuit theory in terms of circuit analogues can be used to model the electrochemical corrosion process. Such modeling can facilitate understanding and lead to better prediction of corrosion rates and overall corrosion behavior.

The fundamental approach of impedance techniques is to apply a small amplitude sinusoidal excitation signal usually a voltage between 5 to 10 mV which is applied to the working electrode over a range of frequencies, ω of 0.001 Hz to 100,000 Hz. The current is measured. The applied voltage is divided by this measured current. Since both the voltage and current have a sinusoidal component with respect to time and are usually out-of-phase, the division results in the electrochemical impedance Z(ω), which itself has real and imaginary contributions. Often, the current is divided by the surface area and the impedance has the units of ohm-cm^2. The electrochemical impedance Z(ω), is the frequency dependent proportionality factor that act as a transfer function by establishing a relationship between the excitation voltage signal and the current response of the system shown in equation (2.14).

$$Z(\omega) = E(\omega)/I(\omega) \qquad (2.14)$$

The magnitude of the resistance or opposition to the current created by capacitors and inductors is dependent on the frequency while the magnitude of the opposition created by the resistor is independent of frequency.

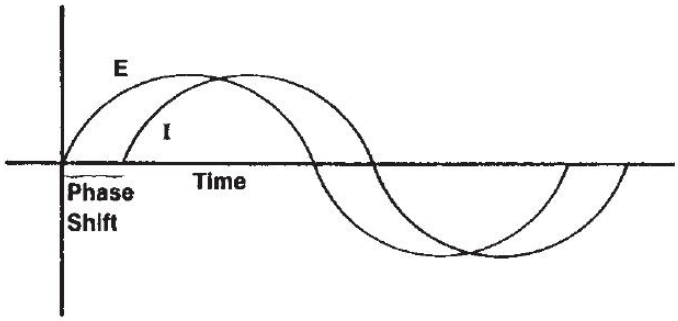

Figure 2.1: Sinusoidal AC voltage and current signals

The technique can be described in terms of a response to a frequency dependent input signal. When a voltage sine or cosine wave is applied across a circuit composed of a resistor only, the resultant current is also a sine or cosine wave of the same frequency with no phase angle shift but with an amplitude which differs by an amount determined by the proportionality factor. In contrast, if the circuit consists of capacitors and inductors, the resulting current not only differs in amplitude but is also shifted in time. It has a phase angle shift. This phenomenon is shown in Figure 2.1.

Vector analysis can be used to describe the equivalent circuit in mathematical terms. The relationship between such vector analysis and imaginary or complex numbers provides the basis for electrochemical impedance analysis. A sinusoidal current or voltage can be viewed as a rotating vector as shown in Figure 2.2. It shows that the current vector rotates at a constant angular frequency f (hertz) or v (radians/s = 2πf). The x component defines the in-phase current. Therefore, it becomes the "real" component of the rotating vector. The y component is shifted out-of-phase by 90°. By convention, it is termed the "imaginary" component of the rotating vector.

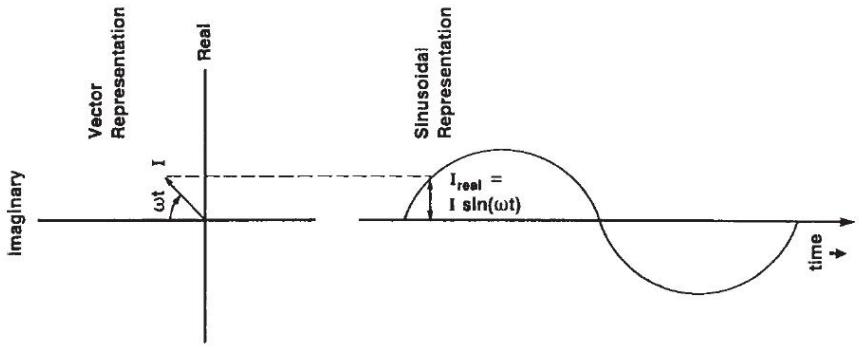

Figure 2.2: Relationship between sinusoidal AC current and rotating vector representation

The mathematical description of the two components is described in below equation:

$$\text{Real Current} = I_x = |I| \cos(\omega t) \quad (2.15)$$

$$\text{Imaginary Current} = I_y = |I| \sin(\omega t) \quad (2.16)$$

$$|I|^2 = |I_x|^2 + |I_y|^2 \quad (2.17)$$

The voltage can be pictured as a similar rotating vector with its own amplitude, *E* and the same rotation speed, v.

As shown in Figure 2.3, when the current is in phase with the applied voltage, the two vectors are coincident and rotate together. This response is characteristic of a circuit containing only a resistor. When the current and voltage are out-of-phase, the two vectors rotate at the same frequency, but they are offset by an angle called the phase

angle, θ. This response is characteristic of a circuit which contains capacitors and inductors in addition to resistors.

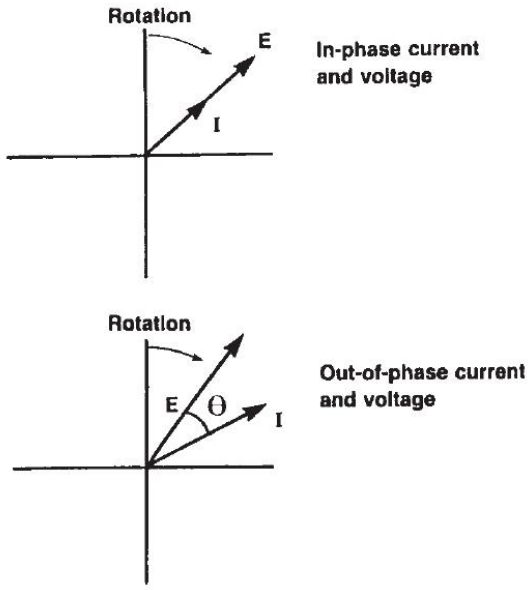

Figure 2.3: In-phase and out-of-phase rotation of current and voltage vectors

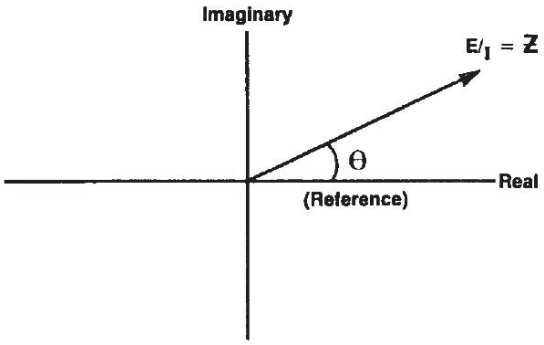

Figure 2.4: Impedance vector

In electrochemical impedance analysis, both the current and voltage vectors are referred to the same reference frame. The voltage vector is "divided" by the current vector to yield the final result in terms of the impedance as shown in Figure 2.4. The impedance is the proportionality factor between the voltage and the current.

The mathematical convention for separating the real (x) and imaginary (y) components is to multiply the magnitude of the imaginary contribution by j and report the real and imaginary values as a complex number. The equations for electrochemical impedance become:

$$E = E_{real} + E_{imaginary} = E' + jE'' \quad (2.18)$$

$$I = I_{real} + I_{imaginary} = I' + jI'' \quad (2.19)$$

$$Z = Z' + jZ'' = (E' + jE'') / (I' + jI'') \quad (2.20)$$

$$\tan \theta = Z''/Z' \quad (2.21)$$

$$| Z |^2 = (Z')^2 + (Z'')^2 \quad (2.22)$$

The goal of the electrochemical impedance technique is to measure the impedance Z as a function of frequency and to derive corrosion rate or mechanism information from the values. Use of simple circuit analogues to model the response is one methodology to achieve this goal. The amplitude of the excitation signal must be small enough so that the response is linearly related to the input, that is, the response is independent of the magnitude of the excitation.

Table 2.2: Circuit elements

Element	Equation
Resistor	$Z = R$
Capacitor	$Z = 1/(j\omega C)$
Inductor	$Z = j\omega L$

The three basic circuit elements can be written as shown in Table 2.1. It shows that a resistor has a real contribution only. That is, the response of a resistor would be a point on the real axis, independent of frequency. Both the capacitor and inductor have purely imaginary contributions. These would appear on the imaginary axis only. One method of electrochemical impedance analysis is to model the corrosion process in terms of circuit elements such as those shown in Table 2.1 and from that model to make conclusions about the physics of corrosion.

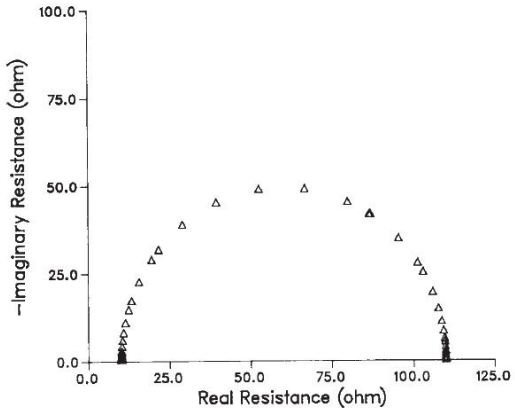

Figure 2.5: Nyquist plot

The plot of the real part of impedance against the imaginary part gives a Nyquist plot as shown in Figure 2.5. The advantage of Nyquist representation is that it gives a quick overview of the data and one can make some qualitative interpretations. While plotting data in the Nyquist format, the real axis must be equal to the imaginary axis so as not to distort the shape of the curve which is important in making qualitative interpretations of the data.

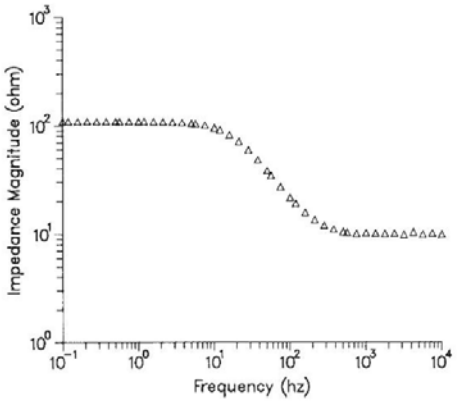

Figure 2.6: Impedance vs. frequency

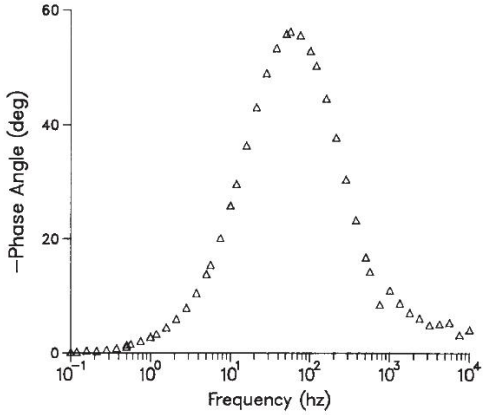

Figure 2.7: Phase angle vs. frequency

The disadvantage of the Nyquist presentation is that one loses the frequency dimension of the data. One way of overcoming this problem is by labeling the frequencies on the curve. The absolute value of impedance and the phase shifts are plotted as a function of

frequency in two different plots giving a Bode plot, as shown in Figure 2.6 and Figure 2.7.

2.3.2 Simple Corrosion Process

The simplest type of corrosion process would be a combination of a corrosion reaction consisting of two simple electrochemical reactions and a double layer. Corrosion would proceed uniformly on the surface. For example, the corrosion of carbon steel in 1 M sulfuric acid can be considered to fall into this category shown in equation (2.23):

$$Fe + 2H^{+} \rightarrow H_2 + Fe^{+2} \qquad (2.23)$$

This reaction may be represented by a simple resistor. The double layer is created by the voltage change across the interface. On the metal side of the interface, there may be an excess (or deficiency) of electrons. This excess (or deficiency) is balanced on the solution side by oppositely charged ions**.** Some are specifically adsorbed at the surface (inner layer). Others are nonspecifically adsorbed and are hydrated. They extend out into the solution in the diffuse layer. The response of this interfacial structure to varying voltage (for example sinusoidal excitation) can be modeled by a capacitor, the double layer capacitance.

For this simple process, the model circuit shown in Figure 2.8. The circuit consists of a resistor *Rp* in parallel with a capacitor *C.* The entire parallel circuit is in series with another resistor *Rs*. The utility of this model for the frequency response lies in the fact that *Rs* equals the solution resistance not compensated by the potentiostat and *Rp* equals the polarization resistance as long as the measurement is made at the corrosion potential. By combining *Rp* with the Tafel slopes for the half-cell reactions by an equation such as the Stern-Geary equation**,** the corrosion rate can be estimated. Thus, analysis of electrochemical impedance enables the corrosion rate to be estimated rapidly in the absence of uncompensated solution resistance when the measurement is made at the corrosion potential.

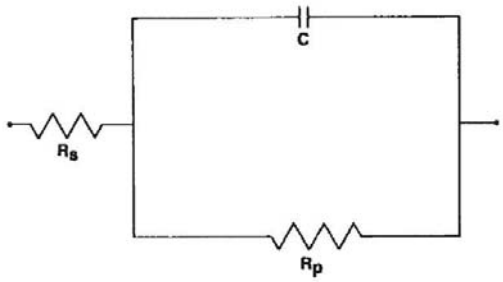

Figure 2.8: Circuit that models simple impedance response

2.3.3 Diffusion Control

Sometimes the rate of a chemical reaction can be influenced by the diffusion of one or more reactants or products to or from the surface. This situation can arise when diffusion through a surface film or hydrodynamic boundary layer becomes the dominating process. Examples are the surface being covered with reaction products of limited solubility. An example of this type of corrosion process that has extreme practical importance is the corrosion of carbon steel in concentrated sulfuric acid in which the product $FeSO_4$ has limited solubility. Such corrosion has been shown to be controlled by the diffusion of $FeSO_4$ from a saturated film at the surface to the bulk fluid**.** Very often, electrochemical impedance data for such systems has a unique characteristic known as the Warburg impedance. In the low frequency limit, the current is a constant 45° out-of-phase with the potential excitation**.** The impedance response should ultimately deviate from this relationship. It will return to the real axis at very low frequencies that may be impossible to measure**.** The equivalent circuit is shown in Figure 2.9.

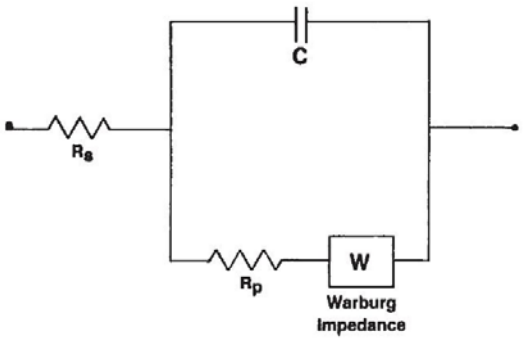

Figure 2.9: Circuit that models impedance in the presence of diffusion

The term *W* is the Warburg impedance. By appropriate manipulation of the data, the values of the circuit elements can be evaluated. These circuit elements can be used to obtain a value for a resistance (charge transfer resistance) that can sometimes be related to a corrosion rate.

2.3.2 Linear Polarization Resistance (LPR)

The electrochemical technique, commonly referred to as Linear Polarization Resistance, is the only corrosion monitoring method that allows corrosion rates to be measured directly, in real time. The polarizing voltage of 10 mV has been chosen as being well within the limits for which the linear relationship between I_{CORR} and $\Delta E/\Delta I$ holds. Additionally, the value is sufficiently small as to cause no significant or permanent disruption of the corrosion process, so that subsequent measurements remain valid.

Anodic and cathodic sites continually shift position, and they exist within a continuously conductive surface, making direct measurement of i_{corr} impossible. Small, externally-imposed, potential shifts (ΔE) will produce measurable current flow (ΔI) at the corroding electrode. The behavior of the externally imposed current is governed, as is that of i_{corr}, by the degree of difficulty with which the anodic and cathodic corrosion processes take place.

Therefore the greater difficulty will give smaller value of i_{corr} and ΔI for a given potential shift. In fact, at small values of ΔE, ΔI is directly proportional to i_{corr}, and hence to the corrosion rate. This relationship is embodied in the theoretically derived Stern-Geary equation:

$$\frac{\Delta E}{\Delta I} = \frac{\beta_a \beta_c}{2.3(i_{corr})(\beta_a + \beta_c)} \qquad (2.24)$$

where βa and βc are the Tafel slopes of the anodic and cathodic reactions respectively.

CHAPTER 3
METHODOLOGY

3.1 Project activities

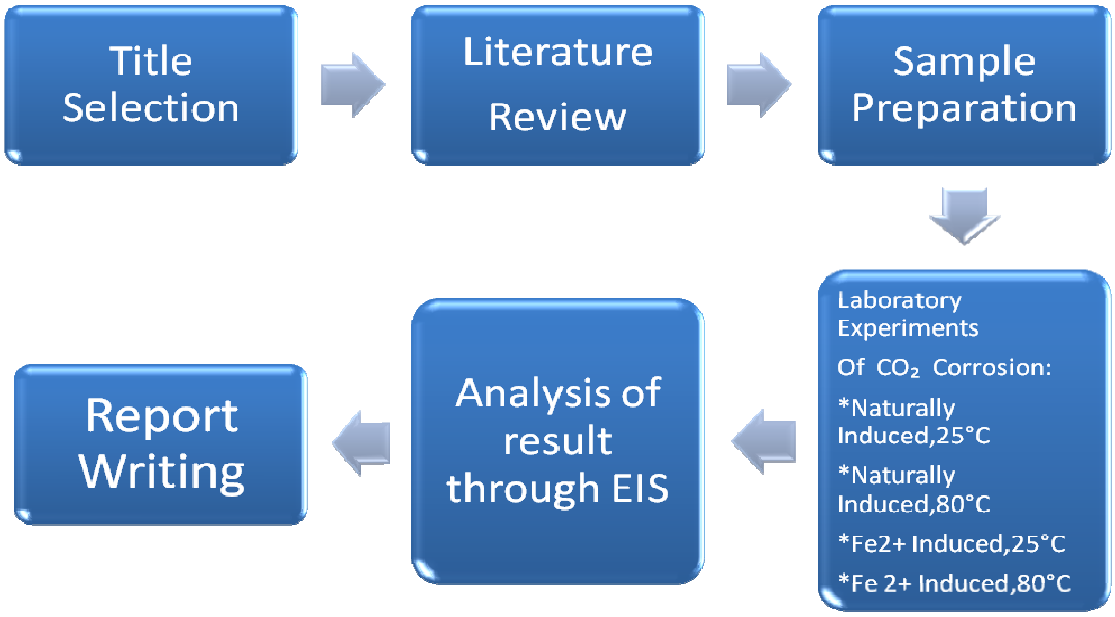

Figure 3.1 Project activities flow chart

From Figure 3.1, it shows the project flow chart where research is done based on books, journals and technical papers specifically on CO_2 corrosion of carbon steel, protective $FeCO_3$ film formation and EIS technique. The laboratory experiments will be conducted using X52 carbon steel in stagnant condition using 3 wt% NaCl over a series of parameters which includes temperature, Fe^{2+} concentration, partial pressure of CO_2 and flow velocity. EIS and LPR techniques are employed to study and analyze CO_2 corrosion rate and formation of protective $FeCO_3$ film layers. Once the results were obtained, analysis was done using SEM technique.

3.2 Electrochemical Measurement Techniques

3.3.1 Electrochemical Impedance Spectroscopy (EIS)

The fundamental approach of EIS technique is to apply a small amplitude sinusoidal excitation signal usually a voltage between 5 to 10 mV which is applied to the working electrode over a range of frequencies, ω of 0.001 Hz to 100,000 Hz. The usual result is a Nyquist plot of half a semi-circle, the high frequency part giving the solution resistance and the width of the semi-circle giving the corrosion rate in the same manner as LPR. The analysis of this data is performed by circle fitting in the analysis software. An advantage of EIS technique is the ability to measure the solution resistance at high frequency.

3.3.2 Linear Polarisation Resistance (LPR)

This technique is based on the linear approximation of the polarization behavior at potentials near the corrosion potential. R_p is given by Stern and Geary equation:

$$Rp = \frac{\Delta E}{\Delta I} = \frac{\beta_A \beta_C}{(\beta_A + \beta_C) i_{corr}} \tag{3.1}$$

$$i_{corr} = \frac{B}{Rp}, \text{ Where } B = \frac{\beta_A \beta_C}{(\beta_A + \beta_C)} \tag{3.2}$$

$ba = 2.3\beta_A$ and $bc = 2.3\beta_c$; $B = babc / 2.3(ba + bc)$

The corrosion current can be related directly to the corrosion rate from Faraday's law:

$$CR(mm/year) = \frac{315xZxi_{corr}}{\rho xnxF} \tag{3.3}$$

Where,

CR = Corrosion Rate (mm/year)

i_{corr} = Corrosion current density, $\frac{\mu A}{cm^2}$

ρ = Density of iron, 7.8 g/cm^3

F = Faraday's constant, 96,500 C/mole

Linear polarization resistance measurements were performed by firstly measuring the corrosion potential of the exposed sample and subsequently sweeping from -10 mV to + 10 mV with the sweep rate 10 mV/min.

3.3 Materials

The material that will be used throughout the experiment is the X52 carbon steel.
The X52 had been purposely obtained from the oil and gas pipeline in order to conduct this project.

3.4 Sample Preparation

The X52 carbon steel pipe is first taken to the manufacturing lab to be cut into smaller pieces. The band saw machine had been used to cut the pipe as shown in Figure 3.2.

Figure 3.2 The band saw machine which cuts the X52 carbon steel pipe

Next, once the steel are in their smaller pieces, the conventional lathe machine (as shown in Figure 3.3) had been used to machine them into the cylindrical shape and had a diameter of 1.2 cm. The abrasive cutting machine had also been used to cut the steel as shown in Figure 3.4.

Figure 3.3 Conventional lathe machining used for turning process

Figure 3.4 Abrasive cutter machine to cut X52 carbon steel

Figure 3.5 The X52 carbon steel which had undergone turning process.

Firstly, the test specimens will be spot welded with copper wire with certain length usually around 30 cm. Then, the test specimens will be mounted with epoxy by cold mounting and grinded with wet silicon carbide (SiC) paper. Finally, the test specimens will be rinsed with deionizer water and degreased with acetone prior to immersion.

3.5 Test Environment

For natural film forming environment, all experiments will be carried out in CO_2 saturated 3% NaCl solution by purging CO_2 for at least one hour prior to each experiment to remove the dissolved oxygen from the test solution. At these conditions

the saturation pH is 3.80. The pH solution can be adjusted by adding an amount of 1M $NaHCO_3$. For induced film forming environment, 50 ppm concentration of ions Fe^{2+} is added to the test solution.

3.6 Experimental Setup

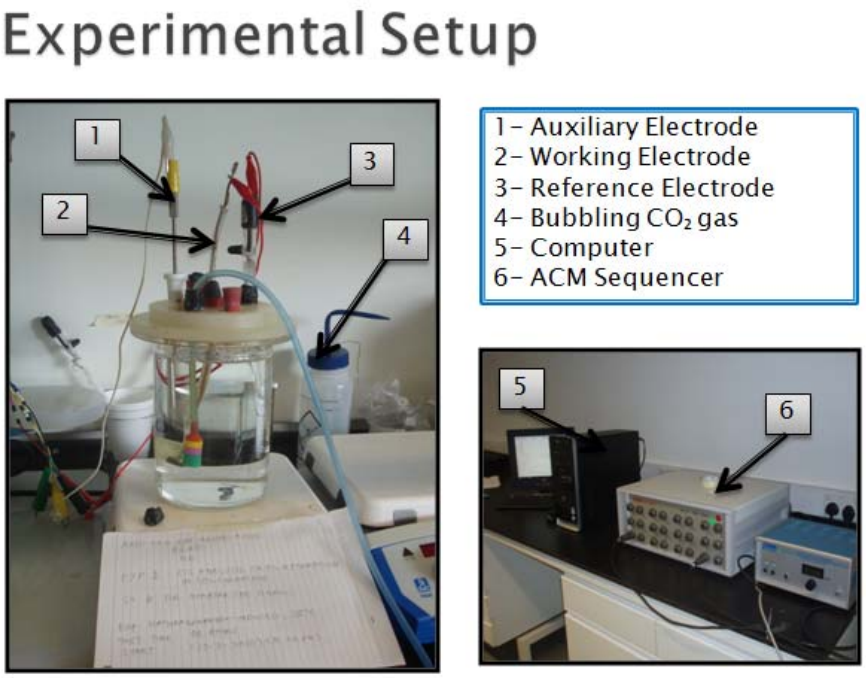

Figure 3.6 Experimental setup

The experimental setup is shown in Figure 3.2. The test assembly consists of one-liter glass cell bubbles with CO_2. The required test temperature is set through a hot plate. The electrochemical measurements are based on a three-electrode system, using a commercially available potentiostat with a computer control system. The reference electrode used is a saturated calomel electrode (SCE) and the auxiliary electrode is a platinum electrode. The test matrix of the experiment is as shown in Table 3.2.

Table 3.2: Test matrix for the research

Parameter	Value
Steel Type	X52 carbon steel
Solution	3 % NaCl
De-oxygenation gas	CO_2
pH	5.5
Temperature (°C)	25°C and 80°C
Fe^{2+} (ppm)	0 and 50
Rotational velocity (rpm)	0 / stagnant
Sand paper grit used	60, 120, 240, 400, 600, 1200, 2400
Measurement techniques	EIS,LPR and SEM

In this project, the effect of temperature (t) = Room Temperature and Fe^{2+}concentration (c_{Fe}^{2+}) = 0 will be specifically studied to observe how these two parameters affect the CO_2 corrosion rate and formation of protective $FeCO_3$ film. The other parameters such as pH, partial pressure of CO_2 and flow velocity will be set at 6.0, 1 bar and 0 rpm / stagnant, respectively. This test matrix is chosen to reflect the conditions in the field. The experiment is conducted for duration up to 96 hours in order to observe the effect of $FeCO_3$ film formation on CO_2 corrosion rate.

3.7 Experimental Procedure

1) Bubble CO_2 through one-litre 3% NaCl for one hour before inserting the sample.
2) Adjust pH of the solution to the required values by adding solution of 1M $NaHCO_3$. pH is measured at room temperature by pH meter.
3) Insert the mounted and polished sample into glass cell and run the experiment
4) For EIS, take readings at the beginning and at the end of the experiment.
5) For LPR, take readings every one hour for 24 hours
6) Repeat the procedures for all temperatures and test environments

CHAPTER 4

RESULTS AND DISCUSSION

The results of natural and induced film formation in CO_2 corrosion environment are presented in Section 4.1 and Section 4.2, respectively.

4.1 Natural Film Forming Environment

All experiments were carried out in CO_2 saturated 3% NaCl solution at pH 5.5 using EIS, LPR and SEM techniques. The immersion time for both of the experiments in the induced film forming environment was maintained for 96 hours.

4.1.1 Electrochemical Impedance Spectroscopy (EIS)

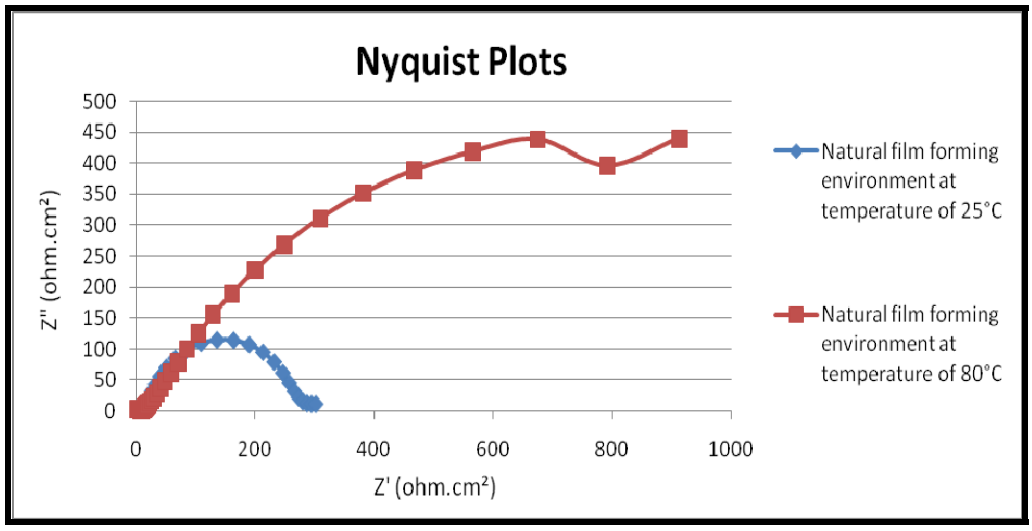

Figure 4.1: Nyquist plot, recorded for 96 hours immersion of a carbon steel specimen in CO_2 saturated 3% NaCl solution at 25°C and 80°C respectively

A selection of typical impedance spectra, presented as Nyquist plots at temperatures of 25°C, and 80°C are presented in Figure 4.1. The Nyquist plots are approximately semicircular, and as the temperature increases, the semicircle's diameter increases,

indicating the decrement in the corrosion rate. This is true for impedance spectra of 25°C, but for impedance spectra at 80°C, it describes the involvement of kinetics and diffusion processes which are inter-related to the formation of $FeCO_3$ film layers. The corrosion rate at 80°C is expected to decrease since $FeCO_3$ film layers are expected to start forming on the steel surface.

Based on the results that have been obtained, these data are later then analyzed using the EIS Analyzer (EISSA). The objective of using EISSA is to interpret the data obtained from the ACM Sequencer in terms of an electrical circuit. There are many types of electrical circuit available for this purpose, nonetheless only the circuit that provides the parameters with the most minimal errors shall be chosen. Among the parameters that would be obtained from EISSA are the R1, R2, P1 and N1. In this case, the CPE electrical circuit is chosen because it provides the most minimal errors. The CPE circuit model and the values obtained from the EISSA are shown below.

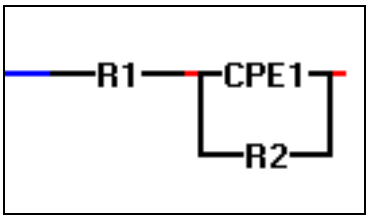

Figure 4.2: The CPE circuit model which is used in the EISSA software

Table 4.1: The values of the respective parameters obtained with EISSA for natural film forming environment

Parameters	Natural Film Forming Environment	
	Temperature = 25°C	Temperature = 80°C
R1	14.5	3.76
R2	261.41	915
P1	0.0005	0.0005
N1	1	1

These values of R_p (obtained from EISSA, Rp= R2-R1) are then used to calculate the average corrosion rate at pH 5.5 of a carbon steel specimen in CO_2 saturated 3% NaCl solution for both temperatures at 25°C and 80°C respectively.

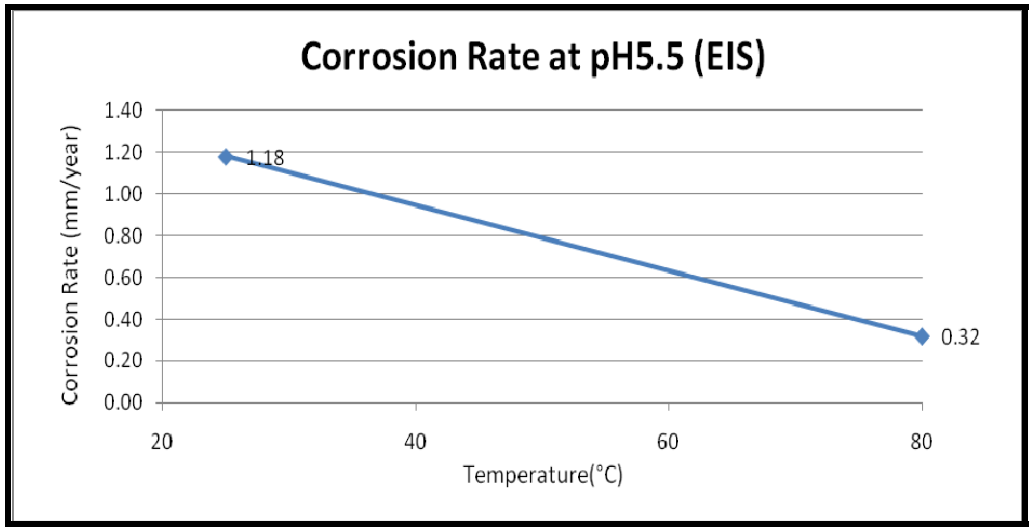

Figure 4.3: Corrosion rate at pH 5.5 (EIS) of a carbon steel specimen in CO_2 saturated 3% NaCl solution at temperatures at 25°C and 80°C respectively

From the results, it shows that the corrosion rate at temperature of 25^{o}C is 1.18 mm/year which then decreases to 0.32 mm/year at temperature of 80°C.

The corrosion rate at temperatures of 25°C and 80°C, in the natural film forming environment can also be explained in terms of the increment of the capacitance double layer (Cdl) values. The Cdl values are obtained through the circle fittings done with ACM Sequencer. According to Lopez [11], consequently, an increment in the capacitance Y values could be related to the growing area of an iron carbonates deposit over the surface samples which are accompanied by an increase in the corresponding Rct values. The growing of the n factor agrees with this assumption because it can be attributed to a decrease of the surface inhomogeneity resulting from the formation of a deposit on the surface.

Table 4.2: Rct, Cdl and corrosion rate values, recorded for 96 hours immersion of a carbon steel specimen in CO_2 saturated 3% NaCl solution at 25°C

Time (hours)	Rct (ohms.cm²)	Cdl (F)	Corrosion Rate (mm/year)
0	1.45E+02	5.60E-04	2.01
48	2.07E+02	1.12E-03	1.41
96	2.59E+02	1.60E-03	1.13

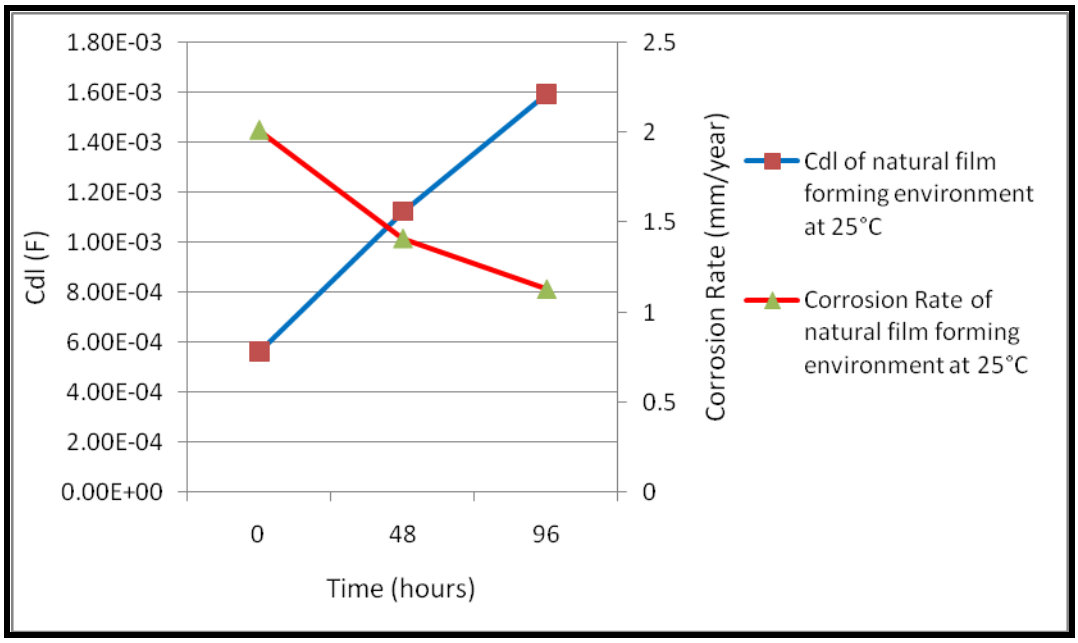

Figure 4.4: Relationship between Cdl, corrosion rate and 96 hours immersion of a carbon steel specimen in CO_2 saturated 3% NaCl solution at 25°C

Referring to figure 4.4, at temperature of 25°C, it is observed that the Cdl value has increased from 5.60E-04 F at 0 hour to 1.60E-03 at 96 hours. Nonetheless, with the increment of Cdl values, the corrosion rate is seen to be decreasing from 2.01 mm/year at 0 hour to 1.13 mm/year at 96 hours.

Table 4.3: Rct, Cdl and corrosion rate values, recorded for 96 hours immersion of a carbon steel specimen in CO_2 saturated 3% NaCl solution at 80°C

Time (hours)	Rct (ohms.cm²)	Cdl (F)	Corrosion Rate (mm/year)
0	8.60E+01	1.00E-03	3.38
48	1.52E+03	2.58E-03	0.19
96	1.50E+03	3.45E-03	0.20

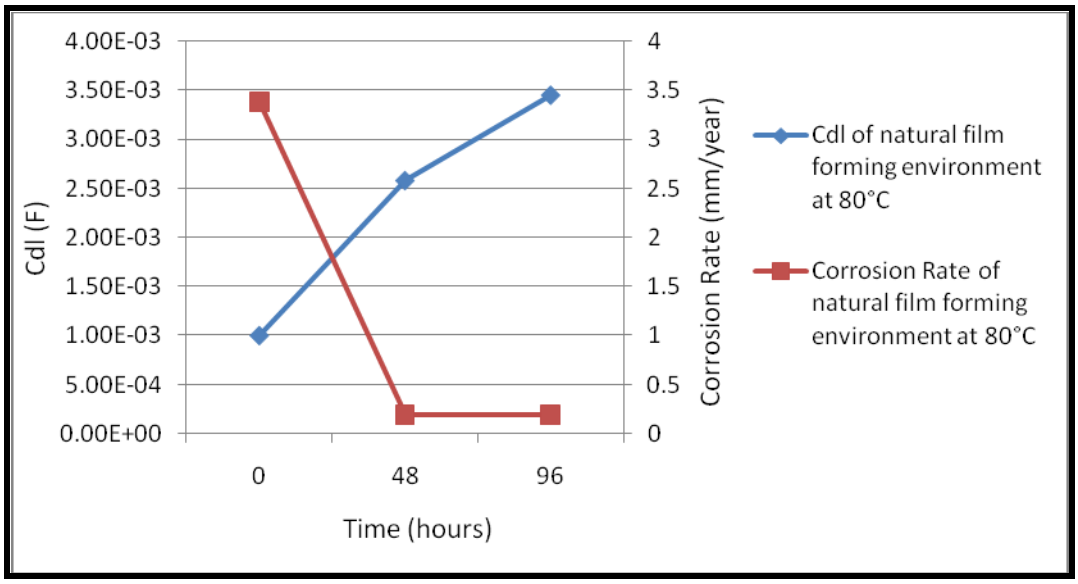

Figure 4.5: Relationship between Cdl, corrosion rate and 96 hours immersion of a carbon steel specimen in CO_2 saturated 3% NaCl solution at 80°C

Meanwhile, referring to figure 4.5, at temperature of 80°C and, it is observed that the Cdl value has increased from 1.00E-03 F at 0 hour to 3.45E-03 at 96 hours. Nonetheless, with the increment of Cdl values, the corrosion rate is seen to be decreasing from 3.38 mm/year at 0 hour to 0.20 mm/year at 96 hours.

4.1.2 Linear Polarisation Resistance (LPR)

Figure 4.6 shows the effect of temperatures to the corrosion rate at pH 5.5 for 96 hours immersion of a carbon steel specimen in CO_2 saturated 3% NaCl solution at

temperatures of 25°C and 80°C. It shows that, after corrosion occurs for several hours, the corrosion rate started to decrease at the 8th hour of the experiment. Besides, it also shows that at low temperatures such as 25°C, the initial corrosion rate is higher compared to the corrosion rate at 80°C, because of the high solubility of the $FeCO_3$ film layers. However, as temperature increases (around 60-80°C), the $FeCO_3$ film layers become more adherent to the steel surface and more protective in nature resulting in a decrease of the corrosion rate. This is due to the, higher temperature increases kinetic of corrosion reaction, makes the solution saturated faster. As such, corrosion rate decreases significantly at temperature of 80°C.

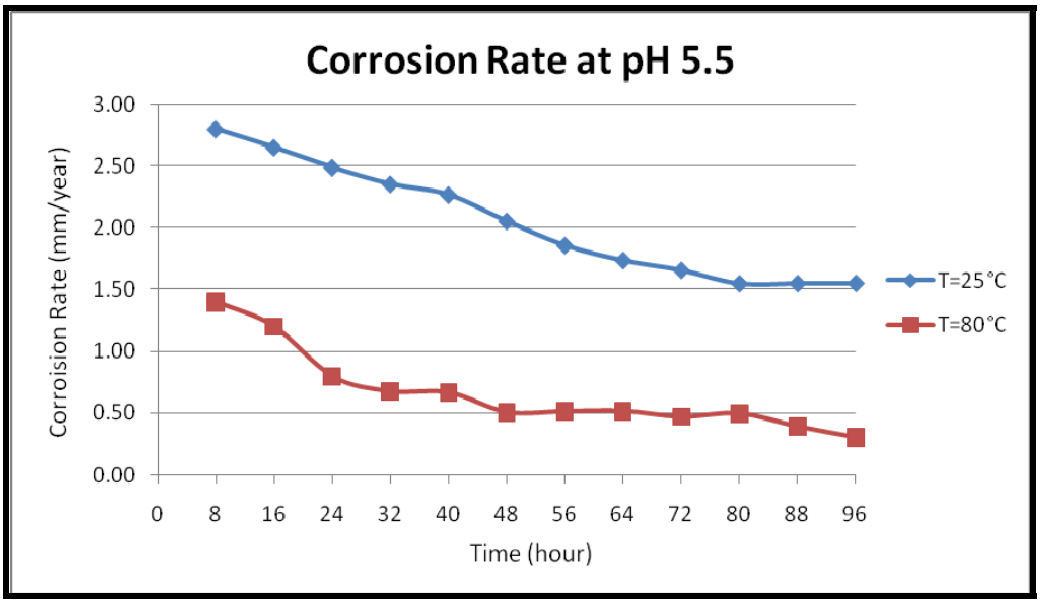

Figure 4.6: Corrosion rate at pH 5.5, recorded for 96 hours immersion of a carbon steel specimen in CO_2 saturated 3% NaCl solution at temperatures of 25°C and 80°C respectively

The corrosion rate at pH 5.5 of a carbon steel specimen in CO_2 saturated 3% NaCl solution for all temperatures is then tabulated into a graph ,by taking the value of the corrosion rate at the end of each experiment. This has been conducted to observe the effect of temperature to the corrosion rate. It is known that increased temperature aids the formation of $FeCO_3$ film layers by accelerating the kinetics of precipitation. From the results, it shows that the corrosion rate at temperature of 25^{o}C is the lowest with

1.55 mm/year while at temperature of 80°C, the corrosion rate decreases to 0.31 mm/year where $FeCO_3$ film layers might have been formed at the steel surface.

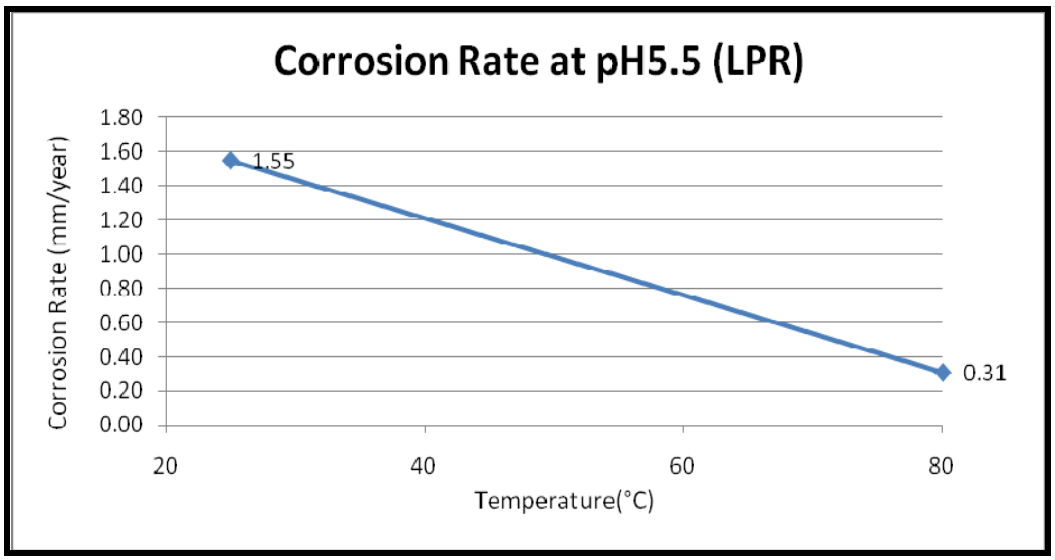

Figure 4.7: Corrosion rate at pH 5.5 (LPR) of a carbon steel specimen in CO_2 saturated 3% NaCl solution at various temperatures of 25°C and 80°C respectively

4.1.3 Scanning Electron Microscopy (SEM)

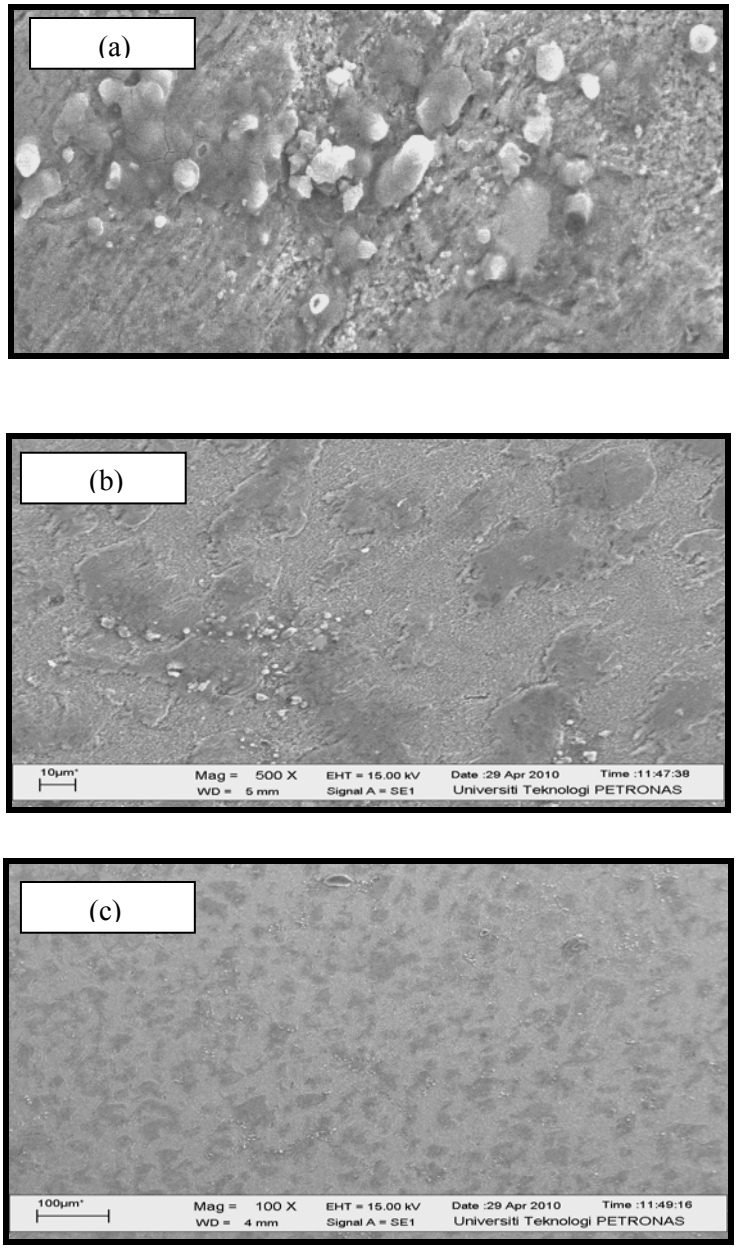

Figure 4.8: SEM images, for 96 hours immersion of a carbon steel specimen in CO_2 saturated 3% NaCl solution at temperature of 25°C (a) 1000x (b) 500x (c) 100x

It can be seen from the SEM images shown in Figure 4.8 that the $FeCO_3$ film layers formed are still porous due to the fact that the experiment was conducted at a temperature of 25°C.

At low temperatures ranges ≥70°C, corrosion rate progressively increases up to an intermediate temperature range (between 70°C to 90°C) after which the corrosion rate diminishes [2]. Crolet [12] had also added, It is thought that the increase in corrosion rate in the low temperature change is due to an increase of mass transfer rate as a result of flow effect and slow $FeCO_3$ formation rate.

According to Kurniawan [6], in obtaining a successful protection, the film must be adherent and cover the whole surface. Temperature strongly influences the conditions needed to form protective iron carbonate layers. At lower temperatures (<60°C) the solubility of $FeCO_3$ is high and the precipitation rate is slow and protective films will not form unless the pH is increased.

In addition, Dugstad [7] has said that the precipitation rate of $FeCO_3$ has been described as slow and temperature dependent process and even under supersaturated conditions, high corrosion rates can maintain for weeks until protective iron carbonate layers are formed, specifically at low temperatures.

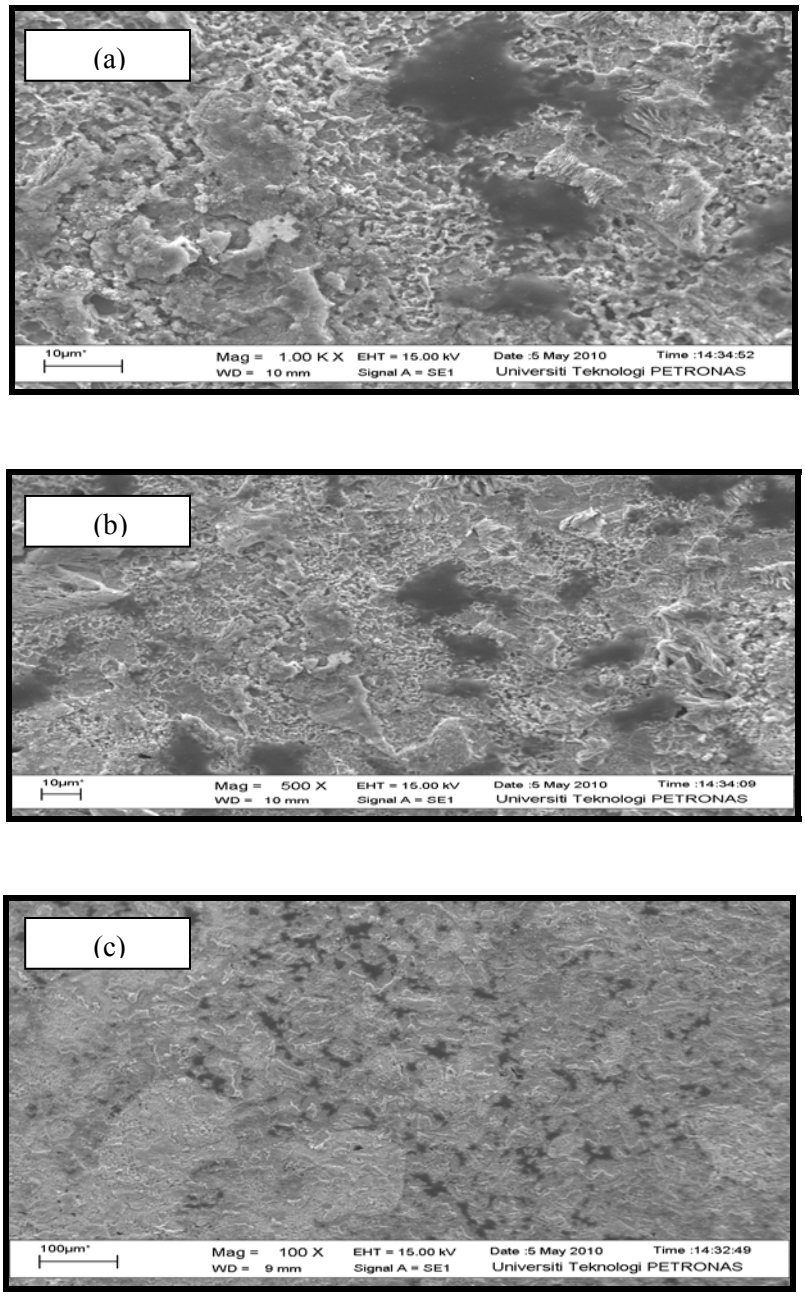

Figure 4.9: SEM images, for 96 hours immersion of a carbon steel specimen in CO_2 saturated 3% NaCl solution at temperature of 80°C (a) 1000x (b) 500x (c) 100x

The SEM images produced at this temperature as shown in Figure 4.9 was undesirable since there was a shortage of CO_2 supply during the experiment. Further investigations should be made and experiments should be reconducted in order to achieve the desired results. Besides that, the SEM test for this sample was postponed for a few days since there was a technical problem (shortage of gas for EDX) with the SEM machine. The sample wasn't properly kept in a decicator, hence, sample might had been oxidized over that period of time.

At higher temperature such as 80°C, the $FeCO_3$ solubility is reduced and the precipitation rate is much faster thus allowing the formations of iron carbonate films. Protective carbonate scales can be recognized already by its morphology and crystallinity. At temperatures ≥ 90°C the scale is composed of well defined and well-packed cubes, while at lower temperatures a flat grain type-appearance is found [7]. Figures 4.10, 4.11 shown below describe the supposed formation of iron carbonate films at temperature of ≥ 90°C [6].

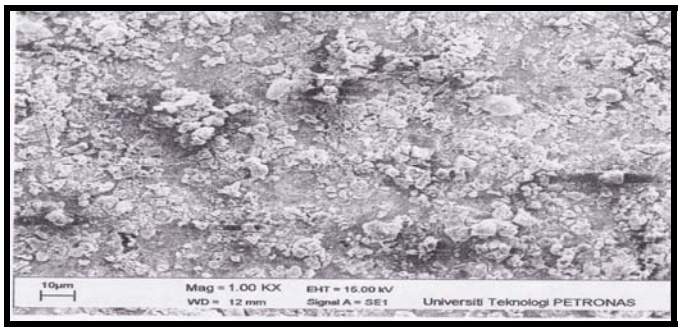

Figure 4.10: Face view of blank CO_2 corrosion after 96 hours showing large amount of $FeCO_3$ film covering steel surface partially.

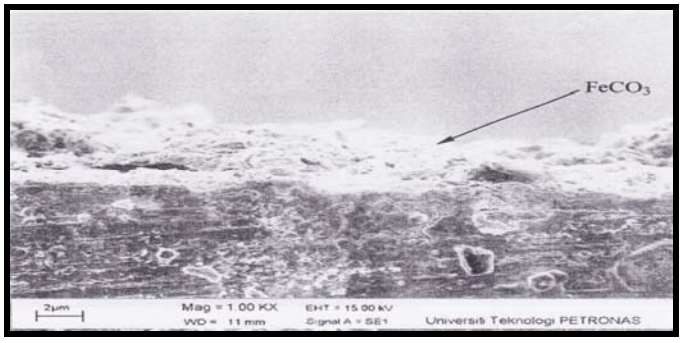

Figure 4.11: Cross section view of blank CO_2 corrosion after 96 hours showing non-uniform thickness amount of $FeCO_3$ film at the steel surface.

4.2 Induced Film Forming Environment

All experiments were carried out in CO_2 saturated 3% NaCl solution at pH 5.5 with an addition of 50 ppm concentration of ions Fe^{2+} to the test solution using EIS, LPR and SEM techniques. The immersion time for both of the experiments in the induced film forming environment was still maintained for 96-hours.

4.2.1 Electrochemical Impedance Spectroscopy (EIS)

Nyquist Plots at temperatures of 25°C and 80°C are presented in Figure 4.12. As shown in Figure 4.9, it can be seen that the diameter of the semicircles have increased significantly as compared to the diameters of the semicircles shown in Figure 4.1. The increment of the temperature causes the corrosion rate to decrease, which simultaneously indicates the possibility of continuous growth of $FeCO_3$ film layers.

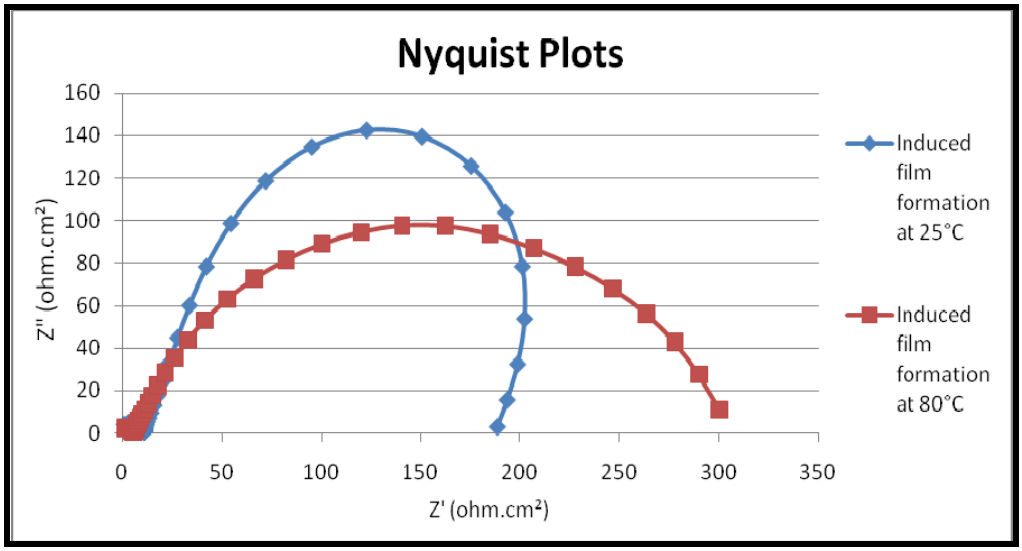

Figure 4.12: Nyquist plots, recorded for 96 hours immersion of a carbon steel specimen in CO_2 saturated 3% NaCl solution with an addition of 50 ppm concentration of ions Fe^{2+} at temperatures of 25°C and 80°C respectively

Based on the results that have been obtained, these data are then used together with the EIS Analyzer (EISSA). The data are then being interpreted in terms of circuit representation in order to reduce the amount of parameters error obtained from the ACM Sequencer. The CPE circuit model and the values obtained from the EISSA are shown below.

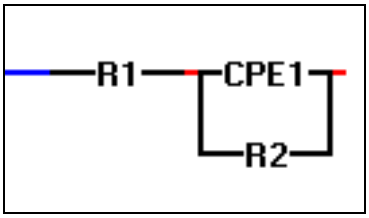

Figure 4.13 The CPE circuit model which is used in the EISSA software

Table 4.4: The values of the respective parameters obtained with EISSA for induced film forming environment

Parameters	Induced Film Forming Environment	
	Temperature = 25°C	Temperature = 80°C
R1	8.5	7
R2	220	300
P1	0.0005	0.00075
N1	1	0.8

From Figure 4.12 the values of polarization resistance, R_p values are obtained from the Nyquist plots. These values of R_p are then used to calculate the corrosion rate at pH 5.5 of a carbon steel specimen in CO_2 saturated 3% NaCl solution with an addition of 50 ppm concentration of ions Fe^{2+} at temperatures of 25°C and 80°C. The corrosion rate is shown in Figure 4.14 below.

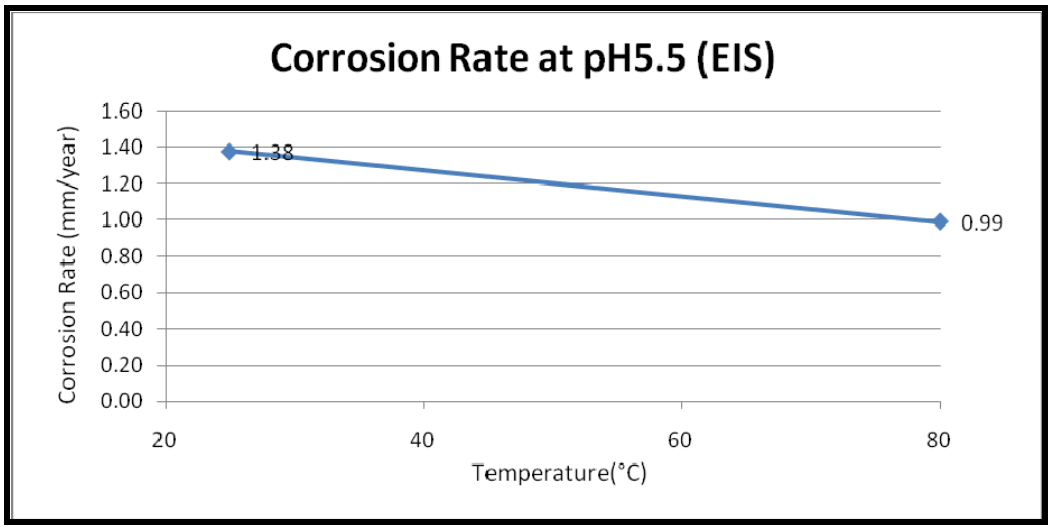

Figure 4.14: Corrosion rate at pH 5.5 of a carbon steel specimen in CO_2 saturated 3% NaCl solution with an addition of 50 ppm concentration of ions Fe^{2+} at temperatures of 25°C and 80°C respectively

From the results, it is observed that at 25°C, the corrosion rate is 1.38 mm/year while at 80°C, the corrosion rate has eventually dropped to 0.99 mm/year prior to the 96 hours of immersion time.

The corrosion rate at temperatures of 25°C and 80°C, in the induced film forming environment can also be explained in terms of the increment of the capacitance double layer (Cdl) values. The Cdl values are obtained through the circle fittings done with ACM Sequencer. According to Lopez [11], consequently, an increment in the capacitance Y values could be related to the growing area of an iron carbonates deposit over the surface samples which are accompanied by an increase in the corresponding Rct values. The growing of the n factor agrees with this assumption because it can be attributed to a decrease of the surface inhomogeneity resulting from the formation of a deposit on the surface.

Table 4.5: Rct, Cdl and corrosion rate values, recorded 96 hours immersion of a carbon steel specimen in CO_2 saturated 3% NaCl solution with an addition of 50 ppm concentration of ions Fe^{2+} at 25°C

Time (hours)	Rct (ohms.cm²)	Cdl (F)	Corrosion Rate (mm/year)
0	1.65E+02	3.47E-04	1.77
48	1.85E+02	6.17E-04	1.58
96	1.95E+02	2.17E-03	1.50

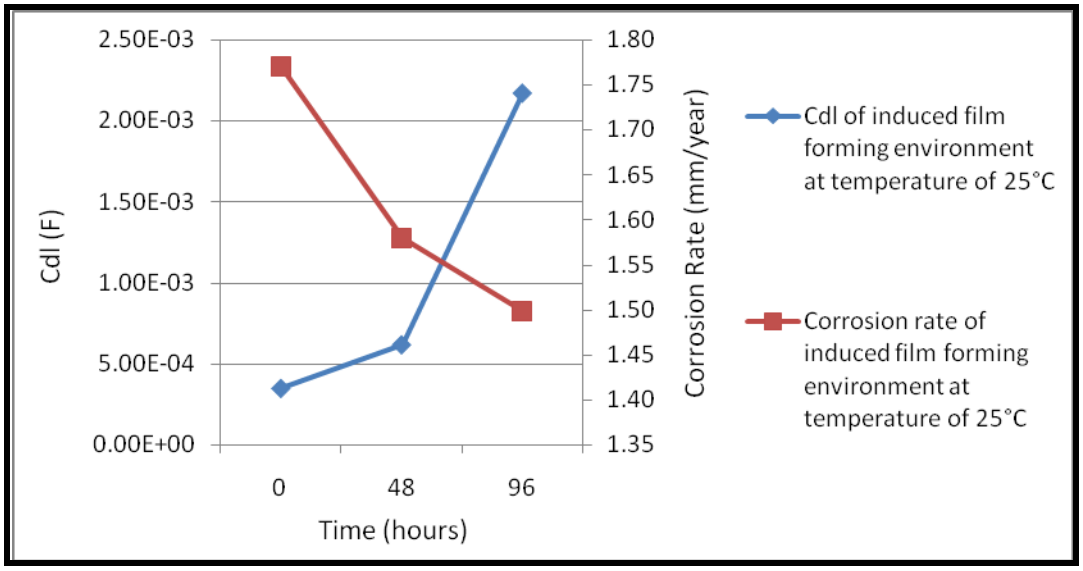

Figure 4.15: Relationship between Cdl, corrosion rate and 96 hours immersion of a carbon steel specimen in CO_2 saturated 3% NaCl solution with an addition of 50 ppm concentration of ions Fe^{2+} at 25°C

At temperature of 25°C and referring to figure 4.15, it is observed that the Cdl value has increased 3.47E-04 F at 0 hour to 2.17E-03 at 96 hours. Nonetheless, with the increment of Cdl values, the corrosion rate is seen to be decreasing from 1.77 mm/year at 0 hour to 1.50 mm/year at 96 hours.

Table 4.6: Rct, Cdl and corrosion rate values, recorded 96 hours immersion of a carbon steel specimen in CO_2 saturated 3% NaCl solution with an addition of 50 ppm concentration of ions Fe^{2+} at 80°C

Time (hours)	Rct (ohms.cm²)	Cdl (F)	Corrosion Rate (mm/year)
0	5.95E+01	1.77E-04	4.95
48	2.30E+02	6.32E-04	1.27
96	3.00E+02	1.03E-03	0.97

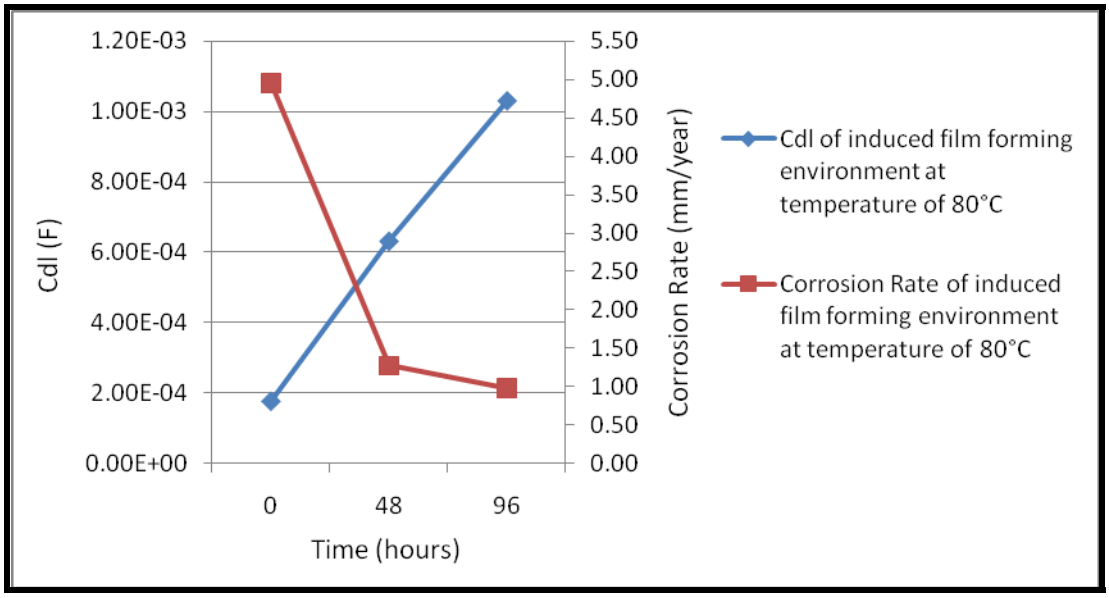

Figure 4.16: Relationship between Cdl, corrosion rate and 96 hours immersion of a carbon steel specimen in CO_2 saturated 3% NaCl solution with an addition of 50 ppm concentration of ions Fe^{2+} at 80°C

Meanwhile, at temperature of 80°C and referring to figure 4.16, it is observed that the Cdl value has increased 1.77E-04 F at 0 hour to 1.03E-03 at 96 hours. Nonetheless, with the increment of Cdl values, the corrosion rate is seen to be decreasing from 4.95 mm/year at 0 hour to 0.97 mm/year at 96 hours.

4.2.2 Linear Polarisation Resistance (LPR)

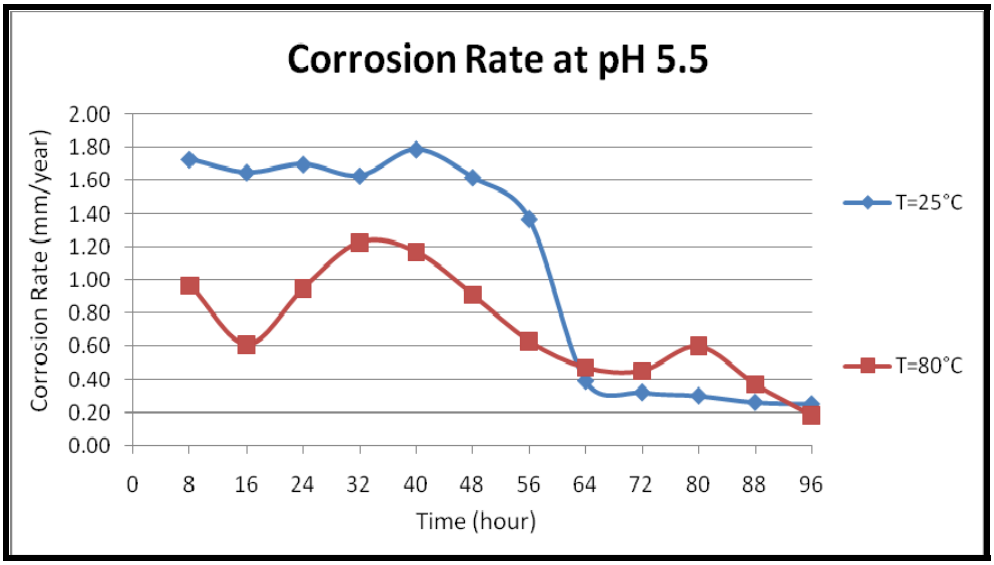

Figure 4.17: Corrosion rate at pH 5.5, recorded for 96 hours immersion of a carbon steel specimen in CO_2 saturated 3% NaCl solution with an addition of 50 ppm concentration of ions Fe^{2+} at temperatures of 25°C and 80°C respectively

Figure 4.17 shows the effect of temperatures to the corrosion rate at pH 5.5 for 96 hours immersion of a carbon steel specimen in CO_2 saturated 3% NaCl solution with an addition of 50 ppm concentration of ions Fe^{2+} at temperatures of 25°C and 80°C. The trends of the corrosion rate are similar to the corrosion rate trends of natural film forming environment but there is further reduction in corrosion rate with the presence of the induced film forming environment. The increase of concentration of ions Fe^{2+} from 0 ppm to 50 ppm, results in higher supersaturation, which consequently accelerates the precipitation rate thus contributing to the formation of thicker $FeCO_3$ film layers. It can be seen from Figure 4.17, that, after corrosion occurs for several hours, the corrosion rate started to decrease smoothly at 96 hours of experiment for both of the temperatures. At temperature of 25°C, the value of the average corrosion rate is high because the kinetics of corrosion reaction is very slow because of the lower temperature. However, at temperature of 80°C, the $FeCO_3$ film layers might have become more adherent to the

steel surface and more protective in nature resulting in a decrease of the corrosion rate. This is because higher temperature increases kinetic of corrosion reaction, makes the solution saturated faster. Therefore, corrosion rate decreases significantly at temperature of 80°C.

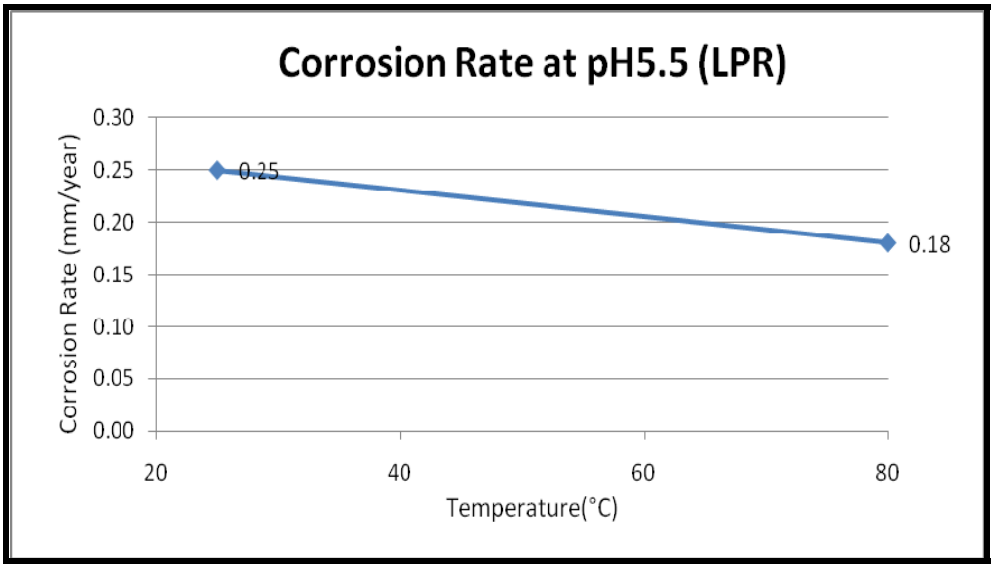

Figure 4.18: Corrosion rate at pH 5.5 (LPR) of a carbon steel specimen in CO_2 saturated 3% NaCl solution with an addition of 50 ppm concentration of ions Fe^{2+} at temperatures of 25°C and 80°C respectively

The corrosion rate is then tabulated into a graph as shown in Figure 4.18 by taking the value of the corrosion rate at the end of each experiment. This is conducted to observe the effect of temperature to the corrosion rate as it is known that increased temperature aids the formation of $FeCO_3$ film layers by accelerating the kinetics of precipitation. The trends of the corrosion rate are similar to the corrosion rate trends of natural film forming environment but there is further reduction in corrosion rate with the presence of the induced film forming environment. From Figure 4.18, the corrosion rate at temperature of 25°C is the highest with corrosion rate of 0.25 mm/year while at temperature of 80°C, the corrosion rate decreases to 0.18 mm/year where thick and dense $FeCO_3$ film layers might have been formed at the steel surface.

4.3 Overall Corrosion Rate

Table 4.7: Corrosion rate for natural film forming environment and induced film forming environment

Temperature (°C)	Corrosion Rate (mm/year)			
	Natural Film Forming Environment		Induced Film Forming Environment	
	EIS	LPR	EIS	LPR
25	1.18	1.54	1.38	0.25
80	0.32	0.31	0.99	0.18

Table 4.7 shows the tabulated data of overall corrosion rate using EIS and LPR techniques for natural film forming environment and induced film forming environment. From the EIS technique, in the natural film forming environment, as the temperature increases from 25°C to 80°C, the corrosion rate decreases from 1.18 mm/year to 0.32 mm/year. In contrast, for the induced film forming environment, the corrosion rate decreases from 1.38 mm/year at temperature of 25°C to 0.99 mm/year at temperature of 80°C. However, the corrosion rate at temperature 80°C should be reinvestigated as it should be smaller than the corrosion rate obtained for the natural film forming environment. Meanwhile, for LPR technique, in the natural film forming environment, as the temperature increases from 25°C to 80°C, the corrosion rate decreases from 1.54 mm/year to 0.31 mm/year. In contrast, for the induced film forming environment, the corrosion rate decreases from 0.25 mm/year at temperature of 25°C to 0.18 mm/year at temperature of 80°C.

CHAPTER 5
CONCLUSION AND RECOMMENDATIONS

5.1 Conclusion

Referring to the results that have been obtained, for natural film forming environment, using the EIS technique, as the temperature increases from 25°C to 80°C, the corrosion rate decreases from 1.18 mm/year to 0.32 mm/year. In contrast, using LPR technique, the corrosion rate decreases from 1.54 mm/year at temperature of 25°C to 0.31 mm/year at temperature of 80°C.

For induced film forming environment, using EIS technique, as the temperature increases from 25°C to 80°C, the corrosion rate decreases from 1.38 mm/year to 0.99 mm/year. On the other hand, using LPR technique, the corrosion rate decreases from 0.25 mm/year at temperature of 25°C to 0.18 mm/year at temperature of 80°C. It has been observed that the corrosion rate is relatively lower in induced film forming environment since the increase of Fe^{2+}concentration results in higher supersaturation, which accordingly steps up the precipitation rate and leads to higher surface scaling tendency and faster formation of $FeCO_3$ film layers which reduces the corrosion rate. Hence, this explains the corrosion rate at temperature 80°C should be reinvestigated as it should be smaller than the corrosion rate obtained for the natural film forming environment

The SEM images of sample at temperature of 80°C were undesirable since there was a shortage of CO_2 supply during the experiment. Further investigations should be made and experiments should be reconducted in order to achieve the desired results. Besides that, the SEM test for this sample was postponed for a few days since there was an unexpected technical problem with the SEM machine. The sample wasn't properly kept in a decicator, hence, sample might had been oxidized over that period of time.

The average corrosion rate is relatively lower in induced film forming environment since the increase of Fe^{2+}concentration fastens the formation of $FeCO_3$ film layers. Referring to the results for both conditions, it shows that for corrosion prediction work, the test is best represented by natural film forming environment. Induced film condition is only suitable for the study in relations to film initiation, growth and propagation.

5.2 Recommendations

Firstly, more test temperatures should be included for experiments in both conditions. Instead of conducting experiments only at temperatures of 25°C and 80°C, perhaps temperatures at 40°C, 45°C, 50°C, 55°C, 60°C, 65°C, 70°C and 75°C should be included. The reason being is that, under certain conditions, a margin of 5°C could result in different corrosion outcome.

Based on the literature review, pH has a strong influence on the formation of $FeCO_3$ film layers. Higher pH fastens the formation of the passive films and therefore, various pH such as pH 6.3 and pH 6.6 should be included in future work.

Parameters like flow velocity should also be taken into consideration. This is because, prior to the formation of $FeCO_3$ film layers, high velocity increases the corrosion rate as Fe^{2+} ions are transported away from the steel surface, thus, leading to a lower concentration of Fe^{2+} ions at the steel surface which later results in a less protective of $FeCO_3$ film formation.

Lastly, it is known that the presence of acetic acid (HAc) also affects the CO_2 corrosion.. By including acetic acid in the study, the relationship between HAc and its role in the CO_2 corrosion, $FeCO_3$ film formation and its protectiveness to a steel surface can be further investigated.

REFERENCES

1. Van Hunnik, E.W.J., Pots, B.F.M and Hendriksen, E.L.J.A. (1996), *The Formation of Protective $FeCO_3$ Corrosion Product Layers in CO2 Corrosion,* Paper No. 6, Houston, Texas: NACE International, Corrosion/1996

2. Kermani, M.B, Morsed, A. (2003), *Carbon Dioxide Corrosion in Oil and Gas Production—A Compendium*, Corrosion Science Vol. 59, Corrosion/2003.

3. Heuer, J.K. and Stubbins, J.F. (1998), *An XPS Characterization on $FeCO_3$ Films from CO_2 Corrosion*, Corrosion Science Vol. 41, Corrosion/1998.

4. Nesic, S., Lee, K.L.J., and Ruzic, V. (2002), *A Mechanistic Model of Iron Carbonate Film Growth and the Effect on CO2 Corrosion of Mild Steel*, Paper No. 02237, Houston, Texas: NACE International, Corrosion/2002.

5. Keddam M., Mattos O.R., and Takenouti H., (1981), *Reaction Model for Iron Dissolution Studied by Electrode Impedance,* J. Electrochem. Soc.

6. Kurniawan, B.A, (2009), *The Effect of Acetic Acid on Film Formation In Carbon Dioxide Corrosion*, Department of Mecahnical Engineering, Universiti Teknologi Petronas, July/2009.

7. Dugstad A., (1998), *Mechanism of Protective Film Formation During CO2 Corrosion of Carbon Steel,* Paper No 31, Houston, Texas: NACE International, Corrosion/1998.

8. Singer, M., Nesic, S. and Gunaltun, Y., (2004), *Top of the Line Corrosion in Presence of Acetic Acid and Carbon Dioxide*, Paper No. 04377, Houston, Texas: Nace International, Corrosion/2004.

9. Johnson M.L and Thomson M.B., (1991), *Ferrous Carbonate Precipitation Kinetics and its Impact on CO2 Corrosion, Paper No. 268,* Houston, Texas: Nace International, Corrosion/1991.

10. Gulbransden, E., (2007), *Acetic Acid and Carbon Dioxide Corrosion of Carbon Steel Covered with Iron Carbonate, Paper No. 07322,* Houston, Texas: NACE International, Corrosion/2006.

11. Lopez D.A, Simson S.N. and Sanchez de S.R., (2002), *The influence of steel microstructure on CO_2 corrosion. EIS studies on the inhibition efficiency of benzimidazole.* Division Corrosion-INTEMA, Facultad de Ingeieria-UNMDP, Juan A.V., Justo B. 4302, B7608FDQ Mandel Plata, Argentina,Corrosion/2002.

12. Crolet J.L, (2002) *Corrosion in Oil and Gas Production* in Corrosion and Anti-Corrosion, eds. Beranger G., Mazille H., (Paris, France: Hermes Science/2002)

APPENDIX: METHOD OF Fe^{2+} ADDITION

1. 100 mL of deionised water (DI water) was deoxygenated in a small beaker for about 15 minutes.
2. 1.78 g of $FeCl_2.4H_2O$ was weighed in weighing dish.
3. $FeCl_2$ was added into the deoxygenated DI water.
4. After $FeCl_2$ was dissolved, the required amount of solution was removed out of the glass cell using a syringe and was added to the test solution by piercing the needle through the septum on the glass cell.
5. The amount of iron chloride solution added to the test solution to achieve a required concentration of Fe^{2+} (ppm), when 1.78 g of of $FeCl_2.4H_2O$ can be calculated using the following steps:
   i. Molecular weight of Fe^{2+} = 56 g/mol

      Molecular weight of $FeCl_2.4H_2O$ = 198 g/mol

      $$\% \text{ of } Fe^{2+} \text{ in } FeCl_2.4H_2O = \frac{56 \text{ g/mol}}{198 \text{ g/mol}} \times 100\%$$

      $$= 28.28\ \%$$

   ii. To prepare solution with 5000 ppm or 0.5% of Fe^{2+}, 1.78 g of $FeCl_2.4H_2O$ was dissolved in 100 mL DI water

   iii. The solution is further diluted by dissolved 1 mL of the solution in step (ii) with 100 mL DI water to achieve 50 ppm of Fe^{2+}
6. The diluted solution containing 50 ppm of Fe^{2+} was always added before the metal sample was immersed in the test solution.